

Development of three-dimensional medium-energy ion scattering using a large solid angle detector

Takane Kobayashi *

RIKEN (The Institute of Physical and Chemical Research), 2-1 Hirosawa, Wako, Saitama 351-0198, Japan

Available online 8 June 2006

Abstract

Three-dimensional medium-energy ion scattering (3D-MEIS) equipped with a large detector has been developed for crystallographic structural and elemental analysis of materials. Backscattering experiments have been made for a Si(001) sample at the geometry that the range of the scattering angle is as large as $\pm 17.5^\circ$. Clear blocking shadows were observed together with belt-like shadow aggregations. A low yield spot not relevant to a blocking cone appears, but it can be excluded from the blocking pattern by changing the detection geometry. The results indicate that 3D-MEIS using a large solid angle detector is promising for crystallographic material analysis.

© 2006 Elsevier B.V. All rights reserved.

PACS: 68.49.-h

Keywords: Structure analysis; Blocking; Position-sensitive and time-resolving detector; Medium-energy ion scattering

1. Introduction

Three-dimensional medium-energy ion scattering (3D-MEIS) has been developed for crystallographic structure and elemental analysis of nanomaterials [1,2]. The system of 3D-MEIS is characterized as that of a pulsed He^+ ion beam with a medium energy of 100 keV used for an incident beam, and projectiles scattered by atoms in a sample are detected by using a three-dimensional detector. The detector consists of two sequentially attached micro-channel plates (MCP) with two delay-line anodes wound perpendicularly to each other. 3D-MEIS spectroscopy provides three-dimensional information; on the spatially two-dimensional blocking pattern of particles scattered from a crystalline sample and, as the third-dimensional information, on flight times of scattered particles. Energies of scattered particles are evaluated from the flight time analysis.

In the usual two-dimensional MEIS, an electro-magnetic energy analyzer is used, and the particle detection ambiguity which arises by the ion neutralization process may be a fatal problem not only for elemental but also for structural analysis [3]. But it is not the case for the 3D-MEIS concerned here. Furthermore, the precise and time consuming adjustment of the sample direction is not necessary even for structural analysis.

In the case of 3D-MEIS using a small solid angle detector, the sample setting angle must be changed several times even for the single surface analysis, since the blocking patterns over the wide range of scattering angle are necessary. However, by using the 3D-MEIS with a large solid angle detector, a blocking pattern over the wide scattering angle range can be obtained at the single setting of experimental geometry. Therefore, a precise structural analysis is carried out with a small error. That is, 3D-MEIS equipped with a large solid angle detector is greatly advantageous.

The development of a 3D-MEIS equipped with a MCP (Roentdek DLD120) of 120 mm diameter has been attempted to the experiments on a sample of Si(001).

* Tel.: +81 48 467 9480; fax: +81 48 462 4709.

E-mail address: tkoba@riken.jp

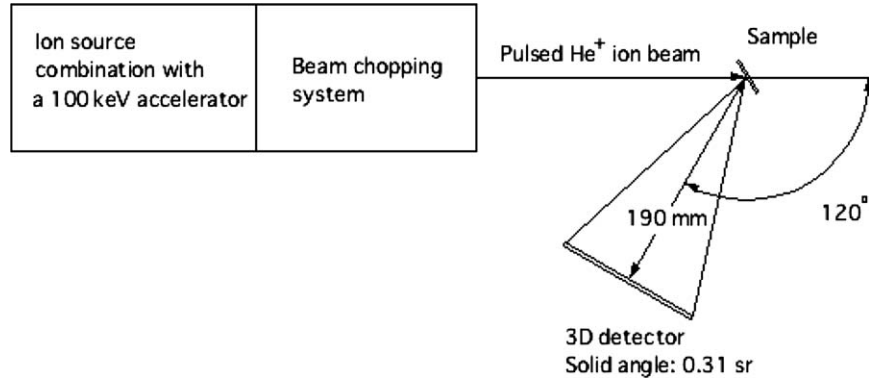


Fig. 1. Schematic of experimental setup. A pulsed He⁺ ion beam with a pulse width of 1.3 ns at a medium energy of 100 keV is used for an incident beam. The detector of scattered particles is the microchannel plate with the diameter of 120 mm. It is claimed to be three-dimensional; position-sensitive (two-dimensions) and time-resolving (third-dimension). The distance between a target and the detector is 190 mm and the solid angle subtended by the detector at this distance is 0.31 sr.

2. 3D-MEIS system using a large solid angle detector

The 3D-MEIS system consists of four sections; an ion source in combination with a 100 keV accelerator, a beam chopping system, a sample and a three-dimensional detector. Fig. 1 shows the schematic diagram of the present experimental setup. The incident pulsed ion beam is characterized as follows; the projectile is He⁺ ion, the pulse width obtained from TOF spectra 1.3 ns, the repetition rate set to be 500 kHz and the beam size of 0.5 mm × 1 mm, respectively. The detector is a position-sensitive and time-resolving microchannel plate (MCP) detector (Roentdek DLD120). It has two delay-line anodes perpendicularly wound (*x*- and *y*-directions) to each other. A time-to-digital converter (TDC) (Roentdek HM1) is used for measurement of the time intervals between a common-start signal from the pulse generator for generating a pulsed ion beam and four stop signals appearing at the 4 ends of the two delay-line anodes. The assignment of the point (*x*, *y*) of the detector on which a scattered particle impinges is carried out from time differences of stop signals appearing at two ends of each delay-line anode. The flight time of scattered particle is evaluated from the summation of time intervals between the common-start signal and the 2 (*x* or *y*) stop signals. The time resolution of the TDC is 150 ps and the maximum counting rate of the TDC is 18 kHz. The count rate of the detector when the beam is not incident on the sample is negligibly small as compared with that during actual 3D-MEIS experiments. When the distance from a beam impinging point on the sample to the detector is 190 mm, the solid angle subtended by the detector is 0.31 sr.

The depth *t* at which projectiles are scattered by atoms of the sample Si(001) is approximately given by

$$t = \frac{K(\theta)E_0 - E_1}{\left(\frac{K(\theta)}{\cos \theta_1} \frac{dE}{dx} \Big|_{E_0} + \frac{1}{\cos \theta_2} \frac{dE}{dx} \Big|_{K(\theta)E} \right)}, \quad (1)$$

where $K(\theta)$ is the kinematics of the scattering at the scattering angle of θ , E_0 the incident energy of the projectile

before entering the sample, E_1 the emerging energy of a particle scattered at a depth *t*. θ_1 and θ_2 are, respectively, the incident angle of the beam and the emerging angle of the scattered particle, with respect to the normal of the surface. $\frac{dE}{dx} \Big|_E$ is the energy loss in Si at the energy of E [4,5]. E is approximately given by

$$E = E_0 - \frac{t}{\cos \theta_1} \frac{dE}{dx} \Big|_{E_0}. \quad (2)$$

An approximate value of *t* is given by setting E in Eq. (1) to be E_0 , and the approximation is improved by using the value of E obtained from Eq. (2). The scattering angle θ is given by $\theta = 180^\circ - \theta_1 - \theta_2$.

In the case at $\theta_1 = 30^\circ$ and $\theta = 90^\circ$, the depth resolution with the detector at a distance of 190 mm is calculated from the time resolution to be about 4 nm.

3. Results

A 3D-MEIS image observed at the present experiment is shown in Fig. 2. The location on the detector is assigned from the values of the horizontal (*x*) and vertical (*y*) axes, which are given by the arrival time differences of the stop signals on two ends of each delay-line anode. The color tables at the right of Figs. 2–4 indicate the number of counts per pixel. The range of the scattering angle θ is $120 \pm 17.5^\circ$ with the experimental geometry. Since the position resolution of the detector is less than 0.1 mm, the angular resolution of the 3D-MEIS system at a distance of 190 mm is less than 0.03° . This angular resolution is sufficient to examine the details of the observed blocking patterns.

Circular shadowed areas labeled by a, b, c, and c' are observed. They are, respectively, originated from the blocking cones of Si(114), (112), (123) and (213) axes. Several belt-like shadowed areas are observed. The horizontal ($y = 0$) and the vertical ($x = 21$) ones are caused by the aggregations of blocking cones from atomic planes of Si{110} and {211}, respectively.

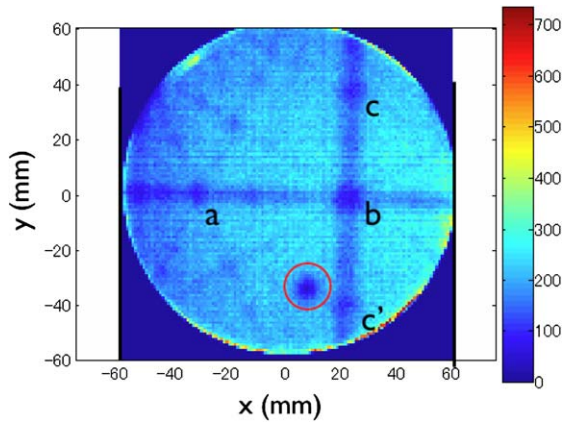


Fig. 2. 3D-MEIS image showing the blocking pattern of He particles scattered from the sample Si(001), where the sampling depth is 5–55 nm. Blocking cones labeled by a, b, c and c' are indexed to the directions of Si(114), (112), (123) and (213) axis, respectively. The horizontal and vertical belt-like aggregations of blocking cones at the positions of $y = 0$ and $x = 21$ are indexed to the Si{110} and {211} planes, respectively. A low yield area indicated by a red open circle appears.

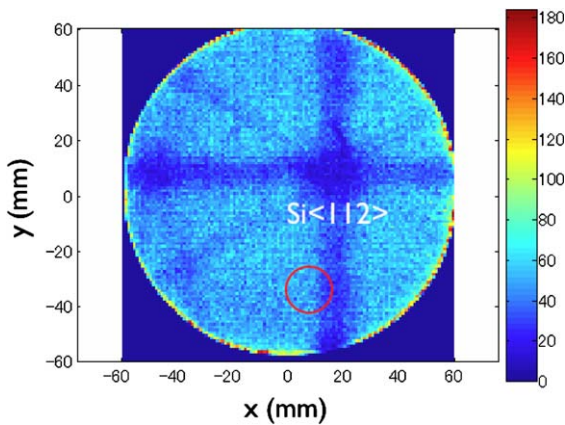
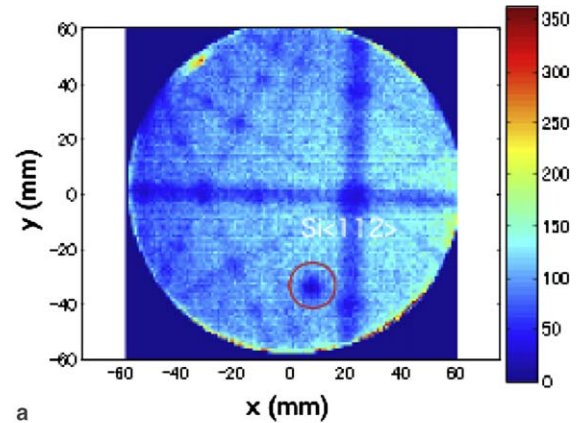
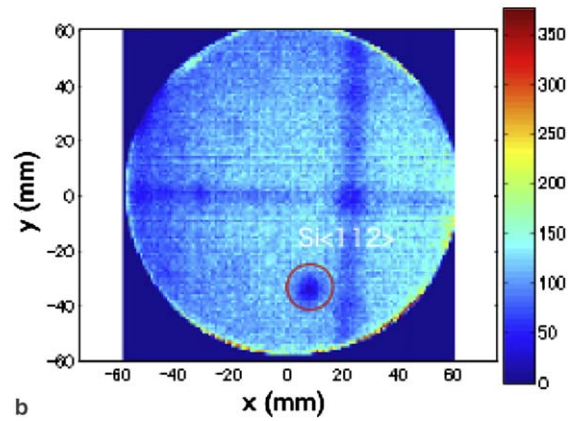


Fig. 3. 3D-MEIS image with the detector at the distance of 360 mm. The blocking cone indexed to the Si(112) direction is observed similarly as in Fig. 2. However, the low yield area is not observed at the position which corresponds to the position labeled by the red circle in Fig. 2.

A low yield area indicated by a red open circle is observed. This is not due to the real shadow cones. Fig. 3 shows a 3D-MEIS image obtained by changing only the distance of the detector from the target to 360 mm instead of 190 mm. The shadowing by the axis of Si(112) is observed, but the shadowing which was expected from the dark spot in Fig. 2 is diminished. This can be explained as follows; scattered particles pass through the channels of the front MCP without collision to the channel walls. This means that the direction of a scattered particle matches with that of the channel of the MCP. Thus, it is possible to exclude such false shadowing by changing the distance between a sample and the detector. Otherwise, MCP with the bias angle is much larger than the declination of the detected particles.



a



b

Fig. 4. Sampling depth dependence of the blocking pattern measured at the distance from the detector to the sample of 190 mm; (a) the blocking pattern due to the sampling at the depth 5–30 nm, (b) that due to the sampling at the depth 30–55 nm. The blocking pattern obtained by the sampling at the shallower depth contains many blocking cones and several belt-like aggregations of blocking cones. However, only few are observed for the sampling at the deeper depth.

In order to investigate the dependence of the blocking pattern on sampling depth at which projectiles are scattered by atoms in the sample, 3D-MEIS images are observed by changing the sampling depth, but the distance between the target and the detector is again 190 mm. The depth is divided into two parts, one is 5–30 nm from the surface, the other is 30–55 nm. Fig. 4 shows the results; (a) from the depth 5–30 nm and (b) 30–55 nm. The blocking pattern from the shallower region includes clear blocking cones and several belt-like aggregations of blocking cones. However, few are observed for the deeper sampling depth. The blocking cones and the aggregations of blocking cones of high indexes seem to be smoothed out. The particles scattered at a depth of 30–55 nm should suffer from similar blocking. Nevertheless traces of the blocking effects on the particles scattered in the high index directions are not observed. It is speculated this is because the scattered particles suffer intense multiple scattering during the outgoing from the depth as shallow as 30 nm and because rather weak blocking effects of axes or planes of high indexes are erased.

4. Summary

3D-MEIS has been developed for crystallographic structural and elemental analysis of materials. A large MCP detector with the diameter of 120 mm has been equipped and 3D-MEIS images have been observed for the target of Si(001), where the solid angle subtended by the detector is 0.31 sr. Blocking patterns over the wide range of scattering angle ($120 \pm 17.5^\circ$) have been observed at the single run; plural and clear blocking cones are observed and precise structural analysis is available from the comparison of such plural blocking cones obtained at a single run.

The dependence of the blocking pattern on the sampling depth in the target was examined. Particles scattered in the high index directions is found to lose traces of the blocking effect. It is speculated this is because the scattered particles suffer from intense multiple scattering during the outgoing from a depth as short as 30 nm, and rather weak blocking effect by the atoms of high indexes is smoothed out.

A false blocking cone is observed at the large solid angle geometry. This is caused by the effect that scattered

particles pass through the channels of the front MCP without collisions on the channel walls. Such false shadowing can be excluded by changing the distance of the detector or by increasing the bias angle of the MCP.

Acknowledgements

The author would like to thank Mr. S. Shimoda, Mr. Y. Oe, Dr. Y. Nakai, Dr. Y. Yamazaki and Dr. A. Koyama for their technical assistance and helpful discussions.

References

- [1] S. Shimoda, T. Kobayashi, Nucl. Instr. and Meth. B 219–220 (2004) 573.
- [2] S. Shimoda, T. Kobayashi, J. Appl. Phys. 96 (2004) 3550.
- [3] T. Kobayashi, G. Dorenbos, S. Shimoda, M. Iwaki, M. Aono, Nucl. Instr. and Meth. B 118 (1996) 584.
- [4] J.F. Ziegler, The Stopping and Ranges of Ions in Matter, Vol. 4, Pergamon, New York, 1977.
- [5] J.F. Ziegler, New Uses of Ion Accelerators, Plenum, New York, 1975.